

Inelastic photoelectron diffraction from Si

E. Puppini

Istituto di Fisica, Politecnico di Milano, Piazza Leonardo da Vinci 32, 20133, Milano, Italy

C. Carbone

*Institut für Festkörperforschung des Forschungszentrums Jülich G.m.b.H., D-5170 Jülich,
Federal Republic of Germany*

R. Rochow

Institut für Angewandte Physik, Universität Düsseldorf, D-4000 Düsseldorf 1, Federal Republic of Germany

(Received 2 March 1992; revised manuscript received 1 June 1992)

We present inelastic photoelectron-diffraction data from Si(100) on the angular dependence of the Si $2p$ peak and its plasmon losses taken by scanning the polar angle from [001] to [110]. The data show that plasmon damping only occurs if the atomic chains that give rise to forward-scattering peaks contain more than three atoms sufficiently close to each other. If, as along the [113] direction, the atoms are arranged in well-separated doublets, the photoelectrons are effectively focused but no defocusing occurs. For this reason, plasmon damping is not observed in this case, whereas it is clearly observed along the [111] direction, where the atoms are closer and defocusing can take place. Finally, we will discuss the angular dependence of the intensity of the spectral region usually labeled as "background" and we will point out the possible connection of our results with the problem of the weight of intrinsic plasmons in photoemission spectra.

INTRODUCTION

In a photoelectron-diffraction (PED) experiment the photoemission intensity of a particular core level is measured versus the emission angle.¹ Interference between the emerging photoelectron wave and the scattered waves gives rise to a diffraction pattern with a series of characteristic intensity oscillations. For kinetic energies above a few hundred eV the emerging electrons are focused along those directions where the sample atoms are aligned (low-index directions): this effect is usually called forward scattering (FS) and can be explained in terms of a simple model based on single-electron scattering. FS has been exploited in the investigation of the structural properties of adsorbate systems, epitaxial interfaces, and magnetic solids.¹ More recently, improved calculations based on multiple scattering (MS) (Refs. 2–4) confirmed this picture but pointed out how MS can cause an effective defocusing by reducing the FS peak intensity expected on the basis of single-scattering calculations. More precisely, a row of 2 or 3 atoms effectively focuses the photoelectrons; the presence of further atoms, however, generates the opposite trend and calculations predict a complete defocusing after 4 or 5 atoms.²

The most convincing experimental evidence of MS effects in PED came from the investigation of the angular dependence of the plasmon-loss intensity.^{5,6} In these studies, it has been observed that both the elastic peak and the plasmon losses are enhanced along low-index directions. However, the strength of the intensity oscillations is maximum for the elastic peak and decreases for successive plasmon losses. For instance,⁵ the elastic Al $2s$ peak from Al(001) generated by FS along the $\langle 011 \rangle$

directions shows intensity oscillation up to 65%; the corresponding first plasmon loss shows 52% oscillations, the second loss 28%, the third loss 21%. This damping has been attributed to a defocusing of the FS maxima produced by the multiple scatterings suffered by the emerging electrons.^{5,6}

In the following, we will present PED data taken from Si(100) on the elastic Si $2p$ peak and its plasmon losses. Since the experiment has been conducted by scanning the polar angle for a fixed azimuth, our diffraction patterns contain several peaks related to different low-index directions. Along these directions plasmon damping is not always observed: we explain this behavior by assuming that plasmon damping depends on various circumstances, such as the average atomic density along each direction and the actual position occupied by the atoms along the chain if they are not simply equally spaced. Our conclusions are in good agreement with results recently obtained by Kaduwela, Friedman, and Fadley,⁷ who developed a computational technique for MS calculations. Finally, we will also discuss the diffraction pattern of the spectral region usually labeled "background" by pointing out its possible connection with the problem of the weight of intrinsic plasmons in photoemission spectra.

EXPERIMENT

The experiment has been performed at the Berliner Elektronenspeicherring Gesellschaft für Synchrotronstrahlung (BESSY) on a HE-PGM (SX-700) beam line.⁸ A VG CLAM electron analyzer was used with an angular acceptance of $\pm 5^\circ$. The experimental apparatus was con-

tained in a conventional vacuum system, base pressure 1×10^{-10} Torr. The Si single-crystal sample was cut from a low-resistivity ($1 \Omega/\text{cm}$), p -type Si(100) wafer. The cleaning procedure consisted in current heating the Si sample. An x-ray-photoemission spectroscopy characterization made it possible to check the cleanliness of the surface which, within the experimental sensitivity, did not show any trace of O or C.

The geometry of our apparatus is shown in the upper part of Fig. 1. The synchrotron-radiation beam and the analyzer axis form a constant 90° angle. The polar angle is scanned by rotating the sample. The azimuthal angle is set along the $[110]$ direction. A series of energy-distribution curves (EDC) normalized to the synchrotron-radiation flux at difference values of the polar angle θ (measured off-normal) have been collected. The intensity of the elastic peak for each value of θ has been measured by evaluating the peak area in the corresponding EDC. A typical I - θ plot for the Si $2p$ elastic peak (kinetic energy 600 eV) is shown in the lower part of Fig. 1; the dotted curve shows the decreasing intensity trend modulated by a series of oscillations. From the point of view of the following discussion, we are more interested in the signal oscillations, namely, in their angular position and intensity. For this reason it is convenient to correct the measured I - θ plots in a way that makes it possible to put in evidence the oscillating component. One possibility is based on the consideration that, due to the experimental geometry, the signal intensity has a decreasing trend roughly proportional to $\cot\theta$ (for θ not too close to 0 and 90° , as it is for the data presented here). Two distinct effects give rise to this behavior. First, the depth of the Si layer sampled with our setup decreases as $\lambda \cos\theta$, λ being the electron escape depth. Second, the area of the sample illuminated by the synchrotron-radiation beam has a surface, seen from the analyzer, that

decreases as $1/\sin\theta$. The I - θ plot corrected by a $1/\cot\theta$ factor is shown in Fig. 1 with a solid line. This kind of correction, which will be adopted for the following discussion, is not relevant *per se*, and will not be discussed in detail. Its purpose is to extract the oscillating component of the signal; in this regard, it is important to note that the same conclusions can be reached by using a different procedure, for instance, by considering the numerical derivative of the I - θ plot or, very simply, by subtracting a linear background from the dotted curve of Fig. 1.

In order to rule out the possible role of surface reconstruction in determining our diffraction patterns, we measured the angular dependence of the ratio between surface and bulk plasmons. This ratio, measured at a kinetic energy of 600 eV, is close to 0.1 for $\theta=70^\circ$, i.e., at the upper edge of our experiment; therefore, it is safe to assume that the weight of a reconstructed surface layer is certainly negligible in determining the diffraction patterns. This observation is consistent with the measured value of the inelastic mean free path for electrons in Si which, at 600 eV, is around 15–20 Å.⁹ A further confirmation of the bulk sensitivity of our data comes “*a posteriori*” from the fact that our diffraction patterns can be directly interpreted in terms of FS along the low-index directions of the bulk crystal (see the next section).

We also measured the diffraction patterns at $h\nu=350$ eV. At this value of the photon energy, the diffraction pattern strongly resembles the one shown in Fig. 1(b). The major difference is a broadening of the FS peaks due to the larger value of the de Broglie length of the photoelectrons. Another minor difference is a small shift (around 5°) of the PED peaks. This shift can be related to true diffraction effects and/or surface reconstruction (the electron mean free path is lower than 10 Å for a kinetic energy of 250 eV). These differences will not be discussed further since they are not relevant to our discussion, mainly focusing on FS which, for a kinetic energy of 600 eV, gives rise to a well-defined and unambiguous diffraction patterns, as shown in the next section.

RESULTS AND DISCUSSION

A typical Si $2p$ EDC ($h\nu=700$ eV) is shown in Fig. 2; the energy window is particularly convenient since, at this photon energy, all the observed spectral features are related to Si $2p$. In fact, on the right-hand side of the elastic peak the signal intensity is negligible, whereas the onset of the Si $2s$ signal is located only 50 eV below the elastic Si $2p$ peak. Surface plasmons, as discussed above, have a negligible weight, and in our data become relevant only for a polar angle higher than 70° , above the upper edge of the investigated range. In the following discussion, the spectrum of Fig. 2 will be divided as shown: we will consider the intensity of the elastic peak (I_0) and of the first and second plasmon loss (P_1 and P_2). Furthermore, we will also consider the spectral region usually classified as background (B).¹⁰ In our experiment we measured a series of spectra like the one in Fig. 2 at 2.5° steps in the polar angle. The I - θ plots show the area of each spectral feature versus the polar angle. As discussed in the experimental section, a $1/\cot\theta$ correction has been

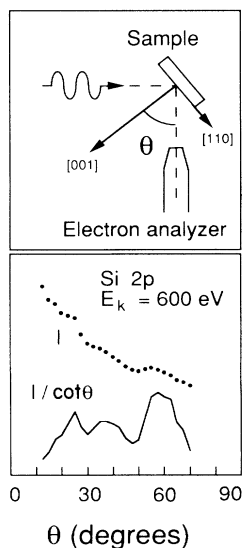


FIG. 1. Top: experimental setup. The polar angle θ is scanned by rotating the sample. Bottom: I - θ plot of the Si $2p$ elastic peak without correction (dotted points) and corrected for the geometric factors (solid line).

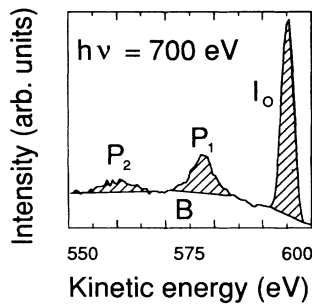


FIG. 2. Si $2p$ energy-distribution curve for Si(100) taken at $h\nu=700$ eV (which corresponds to a kinetic energy of 600 eV). The spectrum is divided into different components: the elastic peak (I_0), the plasmon losses (P_1 and P_2), and the so-called background B .

introduced in order to extract the signal oscillations.

The photoelectron diffraction pattern measured by considering the Si $2p$ elastic peak component (I_0) is shown in the lower part of Fig. 3. The observed structures can be directly related to the low-index direction, as the upper part of the figure illustrates. These directions are also indicated in the lower part of the figure with vertical lines placed at the corresponding angles. The height of each vertical line is proportional to the linear density of Si atoms along the corresponding direction. It is interesting to note the strong correlation between peak intensity and atomic density.

The I - θ plots relative to the different components of the spectrum shown in Fig. 2 are reported in Fig. 4, where the ordinate axis shows the percent deviation of the signal intensity from the mean value. The upper

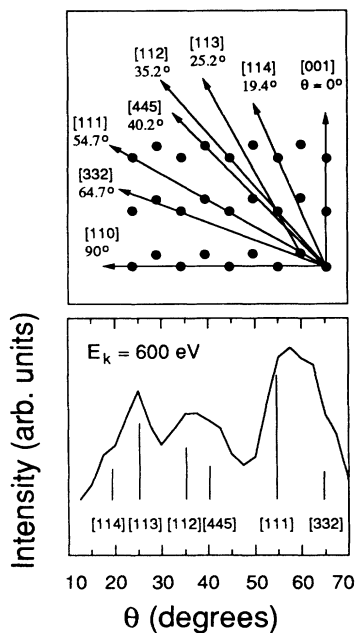


FIG. 3. Top: Si atoms in a $\{110\}$ plane. The low-index directions are indicated with the corresponding off-normal angle. Bottom: I - θ plot of the Si $2p$ elastic peak. The vertical lines indicate the low-index direction. Their height is proportional to the atomic density along the corresponding crystal direction.

panel contains the same curve shown in Fig. 3; the intermediate panels contain the first and second plasmon loss and the lower panel the background pattern. We do not show error bars, since their size would be smaller than the dots used in the figure.

The angular dependence of P_1 and P_2 is clearly the same as that observed in the upper panel for the elastic peak, since a direct correspondence in the peak position exists; the intensity of the PED oscillations, however, strongly depends on the particular peak. This is better observed in Fig. 5, which shows a direct comparison of the raw data without the $1/\cot\theta$ correction introduced in Fig. 4 (as in the dotted line of Fig. 1). Due to the strong difference between the intensity of the various spectral features ($I_0 \approx 3 \times P_1$; $I_0 \approx 9 \times P_2$, see Fig. 2) the original curves have been multiplied by a constant factor with the criterion of having the same absolute value at the lowest angle ($\theta=20^\circ$). The most relevant observation that can be drawn from Figs. 4 and 5 is that the signal oscillation along $[113]$ maintains the same intensity whereas along $[111]$ it decreases. The observed damping along $[111]$ is in good quantitative agreement with the one observed by Osterwalder *et al.*⁵ for the Al $2s$ peaks along the $\langle 011 \rangle$ directions. In the following, we will present a qualitative discussion of this effect with a particular emphasis on the observed difference between $[111]$ and $[113]$. Regarding the structure centered around 35° - 40° , the oscillations appear to be similar for I_0 and P_1 , whereas a reduction is observed in the diffraction pattern of P_2 . Since this structure is actually determined by FS along $[112]$ and $[445]$, a

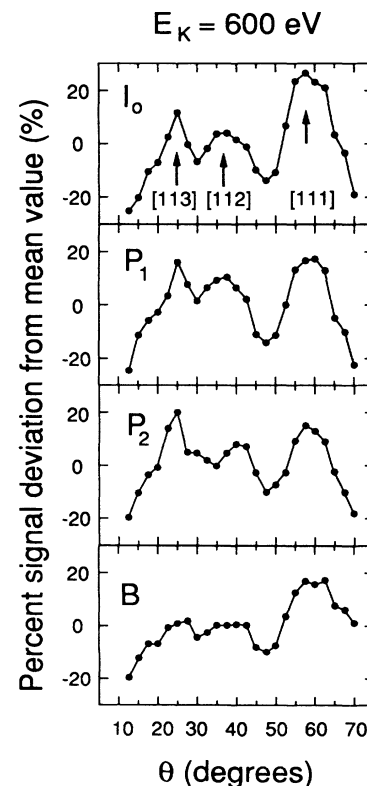


FIG. 4. I - θ plots of the different spectral regions shown in Fig. 2 for an electron kinetic energy of 600 eV.

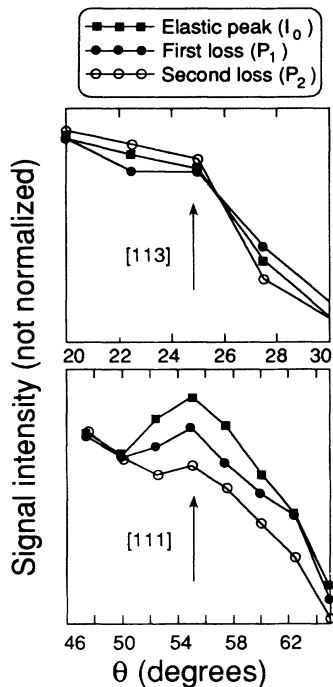


FIG. 5. Comparison of the FS peaks along [113] and [111]. In this figure, the data are presented as measured, i.e., they are not corrected with the $1/\cot\theta$ terms adopted for the data of Figs. 3 and 4. The intensity of the FS peak clearly decreases along the [111] direction, whereas it remains basically the same along the [113] direction.

simple behavior is not expected and, therefore, this point will not be discussed further.

Plasmon damping occurs because the electrons that give rise to the plasmon peaks originate deeper in the sample and, therefore, are subject to defocusing.^{5,6} Our data directly confirm this picture as far as the [111] peak is concerned. It is our opinion that another confirmation comes from the behavior of the [113] peak. The data and calculations presently available on the role of MS effects in PED refer to crystal directions along which the atoms are equally spaced. As already discussed above, calculations for a chain of equally spaced atoms predict that a chain of 2 or 3 atoms is capable of focusing the photoelectrons, whereas with more than 4 or 5 atoms a complete defocusing will occur. In our experiment, the only direction with equally spaced atoms is [112]: on the contrary, in the other directions a basic cell of two Si atoms repeats itself. Along the [113] direction the atoms in the cells are separated by 4.5 Å with a period is 18.0 Å. Along the [111] direction the corresponding values are, respectively, 2.35 and 9.40 Å.

By considering the [113] direction, we can look at the system of the emitting atoms as an array of chains each formed by two atoms. Each doublet produces an effective focusing of the photoelectron, as confirmed by the sharp peak at 25°. However, no defocusing can take place, since the third atom along the chain is placed at a very large distance, 13.5 Å. Also along the [111] direction the Si atoms form separate doublets. However, the separa-

tion between them is much smaller: The distance between the second and the third atom, in fact, is 7.05 Å and the average distance between atoms is only 4.70 Å, which makes this direction the most packed in the [110] planes. For this reason, even though the Si atoms are not simply equally spaced, it is nevertheless reasonable to expect defocusing, as observed in the data.

In summary, our diffraction patterns can be directly interpreted in terms of FS along the low-index directions of the Si sample and the intensity of each FS peak is roughly proportional to the atomic density along that particular direction. By considering the successive plasmon losses, the observed behavior is not the same for the various FS peaks. More precisely, the plasmon damping (i.e., the defocusing effect) is strongly affected by factors such as the average atomic density along the FS direction and also by the details of the atomic positions along the chain. In particular, if the atoms are organized in well-separated doublets, as occurs along the [113] direction, we observe a strong focusing as predicted by the available theories. No defocusing occurs, however, because the next scatterer after each doublet, which will be responsible for this effect, is located too far to be effective. Our conclusions, exclusively based on the analysis of our data, support the conclusions reached by Kaduwela, Friedman, and Fadley in their calculations performed with a MS algorithm.⁷ Hopefully, in the future this computational technique will be applied to the situation discussed in the present paper.

Another issue we investigated is the angular dependence of the so-called background. The polar scan of the spectral region labeled *B* in Fig. 2 is shown in the lowest panel of Fig. 4; clearly, the intensity oscillations of this component follow the oscillations of the elastic peak. The amplitude of these oscillations is reduced with respect to the elastic peak, and the attenuation appears to be slightly stronger for the [113] peak. In the following, however, we will not discuss the details of the background diffraction pattern but we will focus on the fact that *B* gives rise to the same diffraction pattern of the elastic peak.

Aside from the details, the most relevant information is that the *B* component oscillates by closely following the elastic-peak oscillations. The complexity of the problem has been pointed out by Hüfner *et al.*¹¹ The following qualitative considerations can be made regarding the oscillations of the *B* component, even though an explanation is well beyond our present capabilities. The observed diffraction patterns of the elastic peak are, as already observed, due to interference between the photoelectron wave and the other waves scattered by the atoms surrounding the excitation site. The successive excitation, by the photoelectron, of "extrinsic" plasmons (i.e., excited by the photoelectron along its path out of the solid and not related to the core hole, in which case they would be labeled "intrinsic") does not modify the diffraction pattern if, in the plasmon excitation process, the transferred momentum is negligible. This condition is generally satisfied, since the angular spread of the scattered electron after the creation of a single plasmon is on the order of $\Delta E/2E_0$, ΔE being the plasmon energy and

E_0 the initial electron energy.¹² For 600-eV electrons and for $\Delta E = 16.9$ eV, the scattered electrons fall within an angle of $\pm 1^\circ$, small enough to preserve the observed diffraction structures whose widths are on the order of 10° or larger. The low- q plasmons (q being the plasmon wave vector) created in these extrinsic processes have a well-defined energy due to the small dispersion of the plasmon energy in the low- q region. Well-defined plasmon losses of this kind are P_1 and P_2 , whose spectral widths are only determined by lifetime broadening.

In order to explain the origin of region B in terms of plasmon excitation, it would be necessary to invoke the excitation of short-wavelength plasmons, whose energy can be substantially larger compared to the long-wavelength situation due to the relatively large plasmon dispersion observed in Si at high- q values. The plasmon energy in Si along the (100) direction is 16.9 eV for $q = 0$ and increases up to 23.5 eV for $q = 2.4 \text{ \AA}^{-1}$.¹³ (The plasmon lifetime also decreases with increasing q , with a corresponding increase of lifetime broadening.) The extrinsic excitation of such short-wavelength plasmons, however, is unlikely to occur for two reasons. First, this process would probably cancel the forward-scattering peaks due to the large momentum transfer involved in this kind of scattering, and this is not observed. Second, as already discussed, the angular spread of the scattered electrons is small, and this fact indicates that the excitation of short-wavelength plasmon by a traveling electron is a low-rate process. Actually, the plasmon-creation probability decreases as q^{-2} , and this strong decrease makes it difficult, in electron-energy-loss experiments, to observe high- q plasmons.

A possible way to overcome these difficulties is to assume that region B contains a relevant contribution from

intrinsic plasmons. This argument relies on the consideration that the gross features in a PED experiment are mostly determined by the kinetic energy possessed by the photoelectrons at the excitation time. This energy has a well-defined value if the photon energy is completely absorbed by the photoelectron; on the contrary, if the electron sea is left behind in an excited state the electron kinetic energy is spread over a region whose width depends on the plasmon energy. Thus, it is safe to assess that all the photoelectrons give rise to the same diffraction pattern, independently of the loss suffered at the excitation time.

The existence of intrinsic plasmons generated by the sudden creation of a core hole has been experimentally proven by Fuggle *et al.*¹⁴ However, no data or calculations are available on the q distribution of these intrinsic plasmons or on the coupling between the excited-electron sea and the emerging photoelectron. Actually, in literature the estimates of the possible weight of intrinsic plasmons are in strong disagreement; for instance, in the Al $2s$ spectra this weight has been estimated to be between 0% and 50% (Ref. 8) by different authors. Our data point toward a strong weight of intrinsic plasmons; however; this is only a guess that needs more experimental and theoretical confirmations.

ACKNOWLEDGMENTS

This work has been made possible by the financial support of the Ministero della Pubblica Istruzione of Italy through the Consorzio INFM and by the helpful collaboration of the staff of BESSY, in particular, H. Petersen. We would also like to express our gratitude to G. Herman for his valuable advice.

¹For a complete review of PED, see C. S. Fadley, *Phys. Scr.* **T17**, 39 (1987), and references therein.

²S. Y. Tong, H. C. Poon, and D. R. Snider, *Phys. Rev. B* **32**, 2096 (1989).

³M. L. Xu and M. Van Hove, *Surf. Sci.* **207**, 215 (1985).

⁴A. P. Kaduwela, G. S. Herman, D. J. Friedman, C. S. Fadley, and J. J. Rehr, *Phys. Scr.* **41**, 948 (1990).

⁵J. Osterwalder, T. Greber, S. Hüfner, and L. Schlapbach, *Phys. Rev. B* **41**, 12 495 (1990).

⁶G. S. Herman and C. S. Fadley, *Phys. Rev. B* **43**, 6792 (1991).

⁷A. P. Kaduwela, D. J. Friedman, and C. S. Fadley, *J. Electron. Spectrosc. Relat. Phenom.* **57**, 223 (1991).

⁸H. Petersen, *Nucl. Instrum. Methods A* **246**, 260 (1986).

⁹M. Klasson, A. Berndtsson, J. Hedman, R. Nillson, R. Nyholm, and C. Nordling, *J. Electron Spectrosc. Relat. Phenom.* **3**, 427 (1974).

¹⁰E. Puppini, C. Carbone, R. Rochow, and R. Cimino, *J. Electron Spectrosc. Relat. Phenom.* **50**, 353 (1990).

¹¹S. Hüfner, J. Osterwalder, T. Greber, and L. Schlapbach, *Phys. Rev. B* **42**, 7350 (1991).

¹²H. Raether, in *Excitation of Plasmons and Interband Transitions by Electrons*, edited by G. Holer, Springer Tracts in Modern Physics Vol. 88 (Springer, New York, 1980).

¹³J. Stiebling and H. Raether, *Phys. Rev. Lett.* **40**, 1293 (1978).

¹⁴J. C. Fuggle, R. Lässer, O. Gunnarsson, and K. Schönhammer, *Phys. Rev. Lett.* **44**, 1090 (1979).